



## EVALUATION OF ANTIOXIDANT POTENTIAL OF GREEN SYNTHESIZED *TABEBUIA PALLIDA* SILVER NANOPARTICLES

Priyanka Jayachandran<sup>1</sup>, Suganya Ilango<sup>1</sup>, Ramalingam Nirmaladevi\*<sup>2</sup>

<sup>1</sup>Research Scholar, Department of Biochemistry, Biotechnology and Bioinformatics, Avinashilingam Institute for Home Science and Higher Education for Women, Coimbatore, India

<sup>2</sup>Department of Biochemistry, Biotechnology and Bioinformatics, Avinashilingam Institute for Home Science and Higher Education for Women, Coimbatore, India

\*Corresponding author: [nirmaladevi\\_bc@avinutty.ac.in](mailto:nirmaladevi_bc@avinutty.ac.in)

### ABSTRACT

Plant mediated green synthesis of silver nanoparticles has gained much importance in the current scenario. In this study, *Tabebuia pallida* leaves were used as a reducing agent for the sunlight mediated green synthesis of silver nanoparticles. The formation of silver nanoparticles was confirmed by UV-Vis spectroscopy which exhibited absorption maxima at 450 nm which is the characteristic of silver nanoparticles. Further, the characterization of the silver nanoparticles were carried out using Fourier transform infrared spectroscopy analysis, Field Emission Scanning Electron Microscope, Dynamic Light Scattering, and X-ray diffraction analysis. The size of the synthesized silver nanoparticles was found to be ranging between 31.76 nm-50.36 nm and is spherical in shape. The crystalline nature of the synthesized nanoparticles was confirmed by x-ray diffraction. Furthermore, the green synthesized silver nanoparticles were evaluated for their free radical scavenging activity using DPPH Radical Scavenging assay, ABTS radical scavenging assay, Hydroxyl radical scavenging activity, Reducing Power assay and Nitric oxide radical scavenging assay compared with the standard antioxidant Quercetin. Green synthesized silver nanoparticles exhibited a higher antioxidant activity against all the tested free radicals. From this evidences, it could be concluded that the green synthesized *Tabebuia pallida* silver nanoparticles can be used as a potential antioxidant for pharmaceutical applications.

**Keywords:** Antioxidant Activity, *Tabebuia pallida*, Silver Nanoparticles, DPPH Radical Scavenging Activity, Free Radicals.

### 1. INTRODUCTION

Nanotechnology is one of the important disciplines of research in the current scenario. Plants and their derivatives are mainly employed in the synthesis of nanoparticles. Normally the size of the nanoparticles ranges from 1-100 nm [1]. Because of their high surface to volume ratio they possess very good mechanical, chemical and biological properties. Among the various metal nanoparticles synthesized including platinum, copper, gold, and cadmium, silver nanoparticles gained much importance because of their broad spectrum of applications [2].

There are many methods available for the synthesis of silver nanoparticles including radiation, electrochemical, photochemical methods and biological methods. Among these methods, sunlight mediated synthesis of silver nanoparticles gained much importance because this method leads to rapid synthesis of silver nanoparticles

without the help of any instruments. In the field of nanoparticles synthesis, plants are employed and are widely accepted because they are devoid of toxic chemicals and the plants provide various secondary metabolites that act as capping agent and reducing agents which increase the stability of the nanoparticles [3, 4].

Antioxidants are very much important to protect the cells from any kind of degenerative reactions that are caused by free radicals. These antioxidant properties of the plants were attained by the presence of various secondary metabolites including phenols, flavanoids and terpenoids. According to the recent studies, inorganic nanoparticles including silver nanoparticles possess free radical scavenging potential. This might attribute to the various secondary metabolites involved in the reduction and capping of the silver nanoparticles during their formation [5].

*Tabebuia pallida* often called as “Pink trumpet tree” that belongs to the family “Bignoniaceae” is one of the largest genera that is distributed in South America, Central America and Western region of India [6] is the candidate plant of the current study to synthesize the silver nanoparticles.

The main aim of the present study is to carry out sunlight mediated green synthesis of silver nanoparticles from *Tabebuia pallida* and characterize by UV-Vis spectroscopy, Fourier transform infrared spectroscopy (FTIR) analysis, Field Emission Scanning Electron Microscope (FESEM), Dynamic Light Scattering (DLS) and X-ray diffraction (XRD). Furthermore the green synthesized silver nanoparticles were evaluated for their free radical scavenging activity using DPPH Radical Scavenging Assay, ABTS radical scavenging assay, Hydroxyl radical scavenging activity, Reducing Power assay and Nitric oxide radical scavenging assay compared with the standard antioxidant Quercetin.

## 2. MATERIAL AND METHODS

### 2.1. Collection of Plant Species

*Tabebuia pallida* leaves from a place near Avinashi, Tirupur District, TamilNadu was used in the present study for analysis. The plant materials were cleaned many times with running tap water. Consequently the leaves were shadow dried and coarsely powdered, saved in a sealed container for further analysis in laboratory.

### 2.2. Authentication of Plant species

The plant was validated by the Botanical Survey of India [BSI], Southern Circle, Coimbatore. India. Authentication no: BSI/SRC/5/23/2019/Tech./193.

### 2.3. Extraction of the Plant Materials

10 g of the leaf powder was subjected to extraction in 100ml of hydro ethanol solvent (ethanol: water- 60:40) in a Soxhlet apparatus, filtered and stored for further use.

### 2.4. Synthesis of silver nanoparticles:

10 ml of the leaf extract was added to 90 ml of freshly prepared 1 mM silver nitrate solution to attain a final volume of 100 ml. Then it was kept under direct sunlight for 20 mins. Change in color of the solution from brown to dark reddish brown indicated the reduction of  $Ag^+$  to  $Ag^0$ . The solution was then subjected to centrifugation at 15,000 rpm for 45 min. Supernatant was discarded and the pellet that has silver nanoparticles was purified 4 times with deionized water for the removal of leaf extract residue and silver ions. After purification, the

pellet was subjected to lyophilisation and stored in dark for further analysis [7, 8].

### 2.5. Characterization of synthesized silver nanoparticles

The synthesized silver nanoparticles were characterized by UV-visible spectroscopy (Shimadzu Bio Spec-nano), Fourier transform infrared spectroscopy analysis (FTIR spectroscopy- miracle 10, SHIMADZU), Field Emission Scanning Electron Microscope with EDAX (MIRA 3 TESCAN and EDAX APEX), Dynamic Light Scattering (Malvern Instruments, UK) and X-ray diffraction (X'pert Pro X-ray diffractometer).

### 2.6. Evaluation of Antioxidant Activity

#### 2.6.1. DPPH Radical Scavenging Assay

Silver nanoparticles of *T. pallida* were analyzed for their free radical scavenging ability against DPPH radical as stated by the technique of Brand-Williams *et al.*, 1995 [9] with insignificant variations. 0.5 ml of 0.1mM methanolic DPPH solution was combined with 0.5 ml of plant extracts of various concentrations ranging from 25-500  $\mu\text{g/ml}$ . Methanol without DPPH served as the blank and quercetin was used as standard. DPPH in methanol without the samples acted as control. The reaction composition was kept undisturbed for 30 mins in dark condition and later the absorbance was calculated at 520 nm with the help of UV-Vis spectrophotometer. The % scavenging was computed by applying the formula:

$$\% \text{ scavenging activity} = \left\{ \frac{A_c - A_s}{A_c} \right\} \times 100$$

where  $A_c$  - control absorbance,  $A_s$  - sample absorbance

#### 2.6.2. ABTS Radical Scavenging Assay

The antioxidant potential of the samples was determined by employing ABTS radical decolorization analysis as reported by Shirwaikar *et al.*, (2004) [10] with slight modifications. Equal volume of 7mM ABTS and 2.45mM Ammonium Persulfate was mixed 12-16 hours prior to use in dark condition at an ambient temperature. 0.7ml of sample of different concentration was allowed to react with ABTS solution (0.3 ml). The absorbance was calculated at 745nm and the percentage scavenging activity was computed as mentioned earlier.

#### 2.6.3. Hydroxyl Radical Scavenging Activity

The hydroxyl radical scavenging ability of the samples was studied as reported by Klein *et al.*, (1991) [11]. Different concentrations of the samples were mixed with 1.0 mL of iron-EDTA, 0.5 mL EDTA, and 1.0mL of DMSO in 0.1 M phosphate buffer (pH 7.4 ) sequentially

0.5 mL of ascorbic acid was added to commence the reaction and the mixture was kept in a boiling water bath for 15 mins at a temperature of 80-90°C. Thereafter the reaction was terminated by adding 17.5% ice-cold TCA. Then 3mL of Nash reagent was included in the reaction mixture. After 15mins of incubation in an ambient temperature, the absorbance was calculated at 412 nm and the percentage scavenging activity was computed as mentioned earlier. A tube with all these reaction mixtures except the sample serves as the control.

#### 2.6.4. Reducing Power Assay

The assay was carried as reported by Yildirim *et al.*, (2001) [12]. Briefly, various concentrations of sample were combined with 2.5 mL of phosphate buffer (pH 6.6) and 2.5 mL of Potassium ferricyanide then the composition was kept at 50°C for 30 min. After 30 mins, 2.5mL of Trichloroacetic acid was added. Then the mixture was centrifuged at 3000 rpm for 10 min. Equal volume of supernatant and distilled water (2.5 ml) was mixed and 0.5 mL of FeCl<sub>3</sub> was added. The absorbance was calculated at 700 nm.

#### 2.6.5. Nitric oxide Radical Scavenging Assay

The assay was carried out as reported by Shirwaikar and Somashekar, 2001 [13] and Sreejayan and Rao 1997 [14]. 5 mM SNP (Sodium nitroprusside) in 0.025 M PBS pH 7.4 was mixed with varying concentration of the samples and the reaction mixture was incubated at 25°C for 5 hrs. A tube with all these reaction mixtures except the sample served as the control and the buffer alone served as the blank. After 5 hrs of incubation, equal volume of reaction mixture and Griess reagent (0.5 ml) was mixed. The absorbance was calculated at 546 nm.

### 2.7. Statistical analysis

The radical scavenging assays were performed in triplicate and the values are represented as mean ± standard deviation. Statistical significance of the data was analyzed using one-way ANOVA by using Microsoft Excel, 2007 and P value < 0.05 was found to be statistically significant.

## 3. RESULTS AND DISCUSSION

### 3.1. Synthesis of silver nanoparticles

The plant extract of *Tabebuia pallida* was added to the aqueous solution of silver nitrate. After 20 mins of incubation in the direct sunlight, there was a rapid change in colour of the solution from brown to dark reddish brown which indicates the rapid reduction of Ag<sup>+</sup> to Ag<sup>0</sup>

(Fig 1A and 1B). This color change is due to the Surface Plasmon Vibrations excitation in the synthesized silver nanoparticles [15].

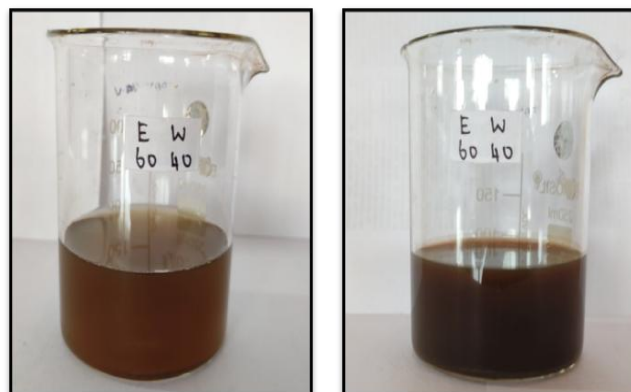


Fig. 1A

Fig. 1B

Fig. 1A: Before exposure to sunlight, Fig. 1B: After exposure to sunlight for 20 mins

### 3.2. Characterization of synthesized silver nanoparticles

#### 3.2.1. UV-Visible Spectroscopy

The silver nanoparticles synthesized using *Tabebuia pallida* leaf extracts were analyzed using UV-Vis spectroscopy to determine the characteristics of the peak spectrum of the silver nanoparticles. Normally the silver nanoparticles appear at the wavelength of 400-600 nm intervals [16]. The Surface Plasmon Resonance of the synthesized silver nanoparticles occur around 450 nm (Fig.2).

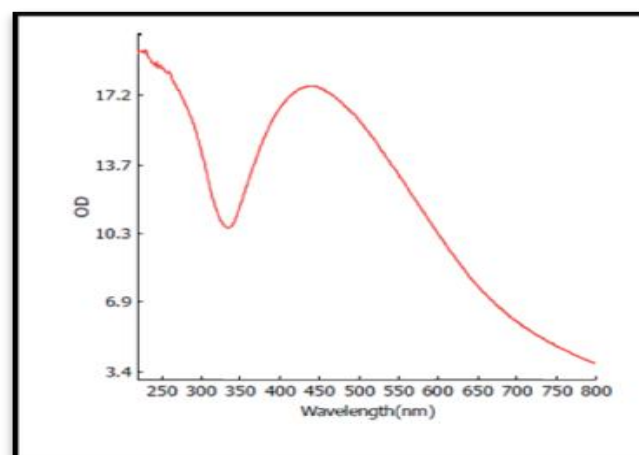


Fig. 2: UV-Visible spectrum of the synthesized silver nanoparticles

Little broadened and a bell shaped peak was formed due to the presence of various secondary metabolites in the plant extract that plays a major part in capping and

reducing mechanism during the formation of silver nanoparticles [17]. According to a theory postulated by Mie, the nanoparticles that are spherical in nature exhibit a single SPR peak. Thus from the above UV-Vis spectrum it is confirmed that the green synthesized silver nanoparticles are spherical in nature [18, 19]. In line with our study Pirtarighat *et al.* (2019), synthesized the silver nanoparticles using the plant extract of *Salvia spinosa* and found that the Surface Plasmon Resonance of the synthesized nanoparticles was at 450 nm [20].

### 3.2.2. Fourier Infrared Spectroscopy Analysis

The metabolites that play a key role in the reduction of silver ions were identified using FTIR spectroscopy. FTIR spectrum of the green synthesized *Tabebuia pallida*

silver nanoparticles is shown in the fig.3. Various peaks in the FTIR spectrum corresponds to the functional groups of various metabolites involved in the reaction. A band at  $601.79\text{ cm}^{-1}$  corresponds to the C-Cl (alkyl halides). Another band at  $678.94\text{ cm}^{-1}$  indicates the presence of =CH of aromatic compounds present in the nanoparticles. A peak at  $2360.87\text{ cm}^{-1}$  corresponds to the symmetric stretching of COO- [21]. Another peak at  $1643.35\text{ cm}^{-1}$  indicates the amide-I from the carbonyl stretch in the amide linkage of proteins [22]. Various peaks at  $3865.35\text{ cm}^{-1}$ ,  $3741.90\text{ cm}^{-1}$  and  $3286.70\text{ cm}^{-1}$  correspond to the hydroxyl (OH) stretching vibration of the alcohol and phenols in the synthesized silver nanoparticles [23].

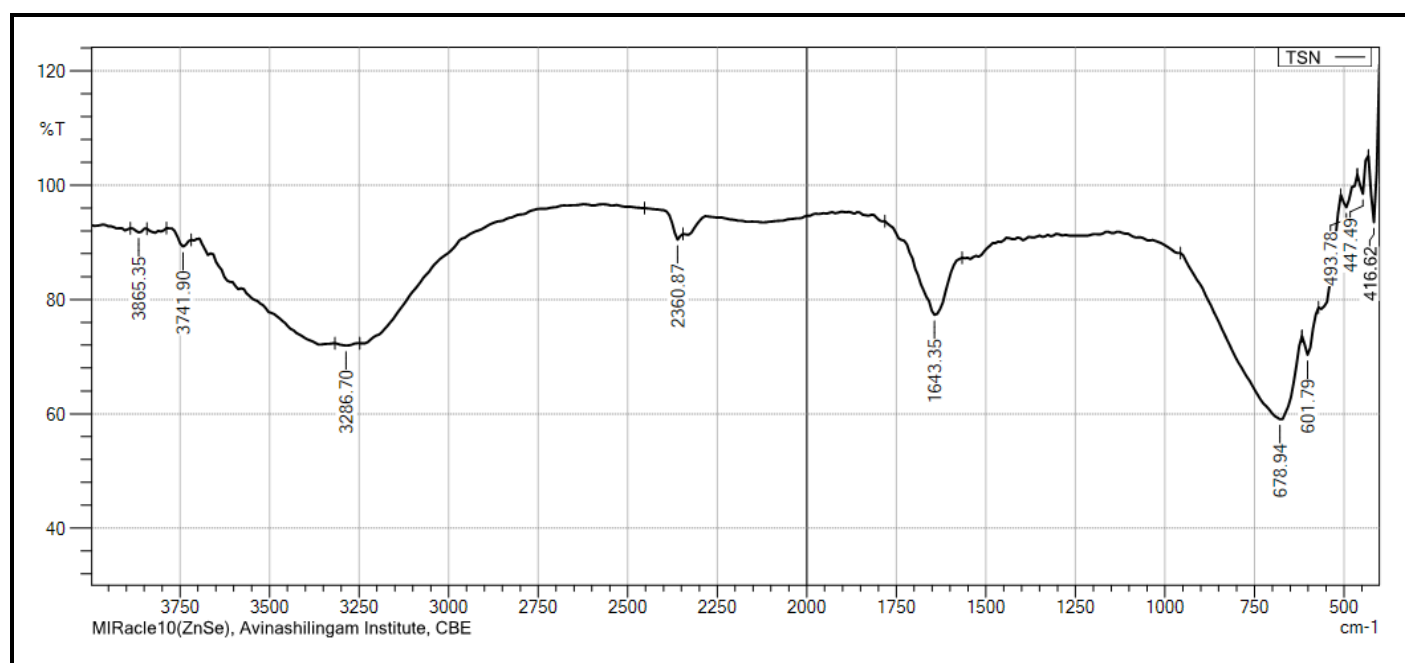


Fig. 3: FTIR Spectrum of synthesized silver nanoparticles

### 3.2.3. FESEM analysis with EDAX

FESEM analysis of the green synthesized *Tabebuia pallida* silver nanoparticles was carried out to analyze the morphology and size. The synthesized nanoparticles were found to be uniformly spherical in shape with the size ranging between 31.76 nm-50.36 nm with least agglomeration and the average size is found to be 38.82 (Fig.4). This difference in particle sizes is due to the involvement of various biomolecules in the synthesis and capping of silver nanoparticles [24]. Similar results were also obtained by Sathishkumar *et al.*, (2012) in the silver nanoparticles synthesized from *Morinda citrifolia*. They found that the size of the synthesized nanoparticles

ranges between 10 to 60 nm and the average size is found to be 27nm [25].

The energy dispersive spectrum of the green synthesized *Tabebuia pallida* silver nanoparticles is depicted in the fig.5 A. A strong peak at 3 KeV indicates the silver nanoparticles because of their Surface Plasmon Resonance [26]. Various elements like Ag, Cl, C, and O are present in the synthesized nanoparticles and their percentage weight is 65.94, 3.52, 15.46, and 15.08 respectively (Fig.5 B). This is one of the biggest advantages over the nanoparticles which are synthesized chemically.

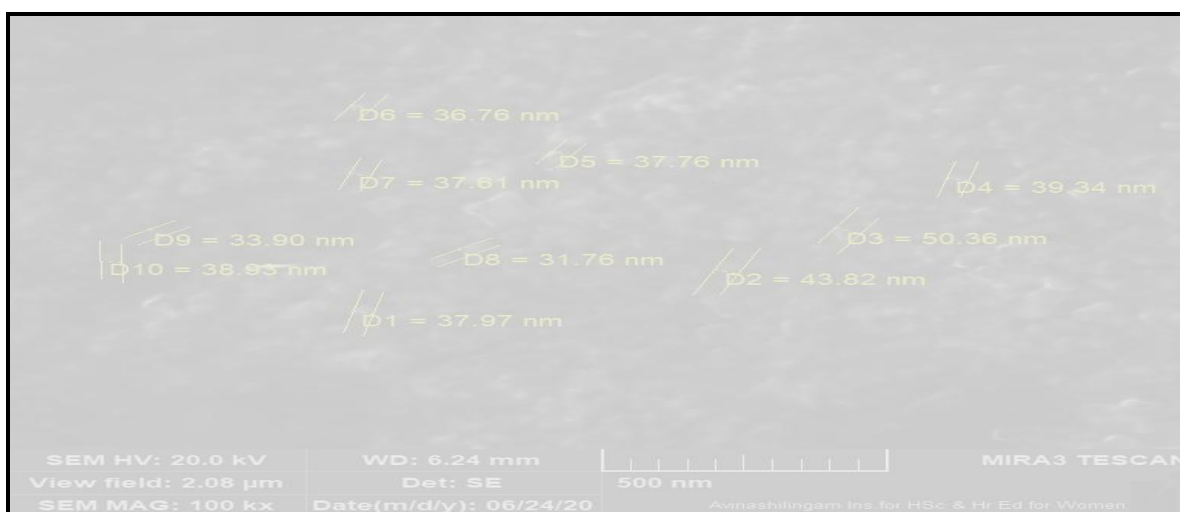


Fig. 4: FESEM Analysis of the synthesized silver nanoparticles

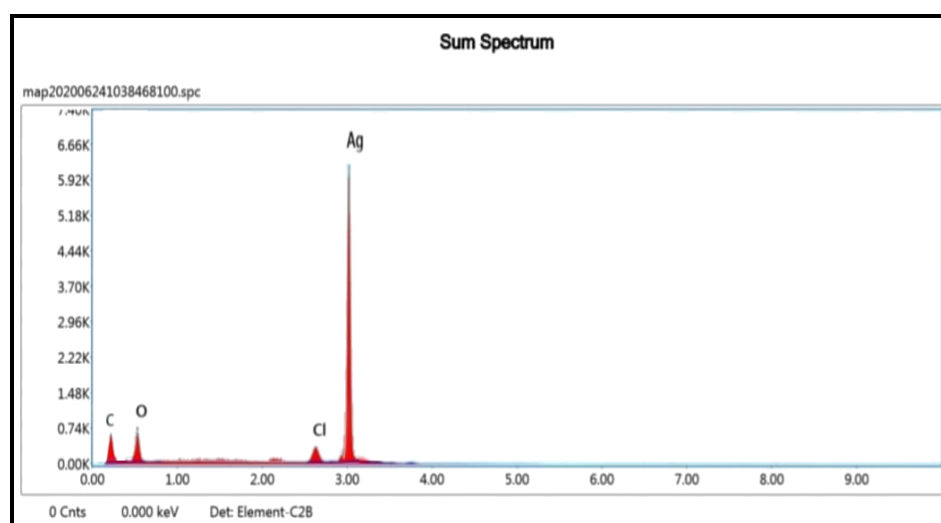


Fig. 5A

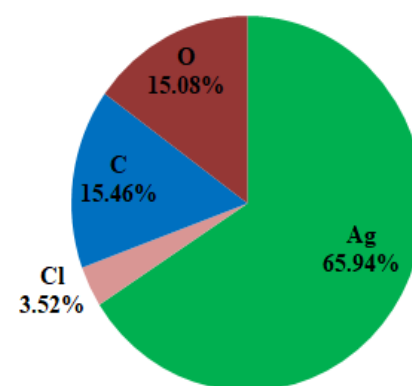


Fig. 5B

Fig. 5A: Energy dispersive spectrum of the silver nanoparticles, Fig. 5B: % weight of various elements in the synthesized silver nanoparticles

### 3.2.4. DLS analysis for particle size and zeta potential

DLS analysis was carried out to determine the particle size, particle distribution index and Zeta potential of the synthesized silver nanoparticles. It is observed that the average size of the nanoparticles was 55.4 nm with a Polydispersity Index (PDI) of 0.33. A single peak obtained in the DLS indicates the purity of the synthesized nanoparticles (Fig. 6A). This obtained size is slightly greater than the size obtained in SEM analysis. This is due to the fact that the SEM only measures the number based size distribution of the physical size and it will not include the capping agent. But the DLS is based on the measurement of hydrodynamic size which

measures diameter of the particle along with the molecules and ions that are attached on the surface of the particle and are in continuous movement in the solution. This makes the size little larger in DLS than SEM [27].

The Zeta potential of the green synthesized silver nanoparticles was found to be -15.6 mV (Fig. 6B). This negative value is due to the presence of negative charge on the outer surface and positive charge on the inner surface of the nanoparticles. From this negative zeta potential it could be confirmed that the synthesized silver nanoparticles were stable for a longer duration since there will be a strong repulsion among the particles that prevents them from agglomeration [28].

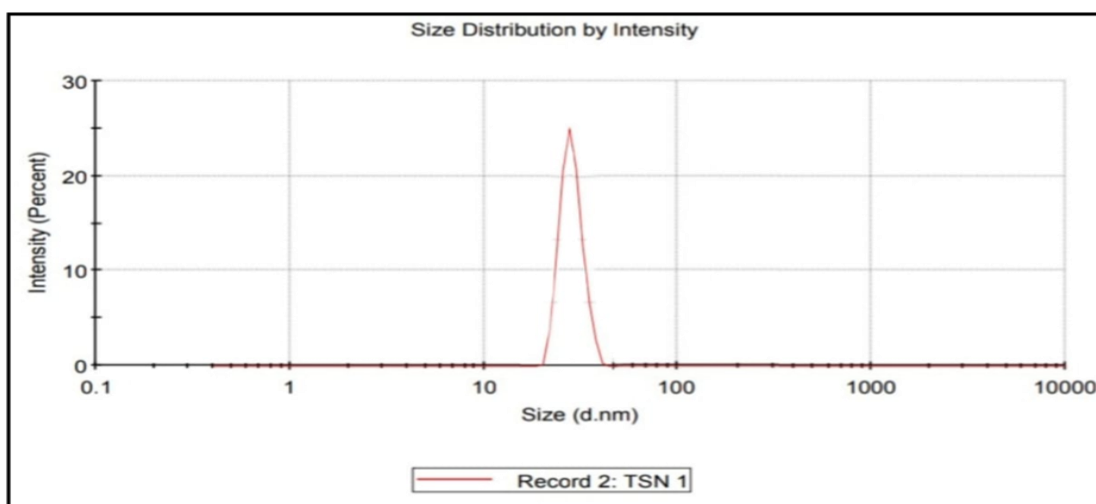


**Fig. 6A:** DLS spectrum of size distribution for the synthesized nanoparticles

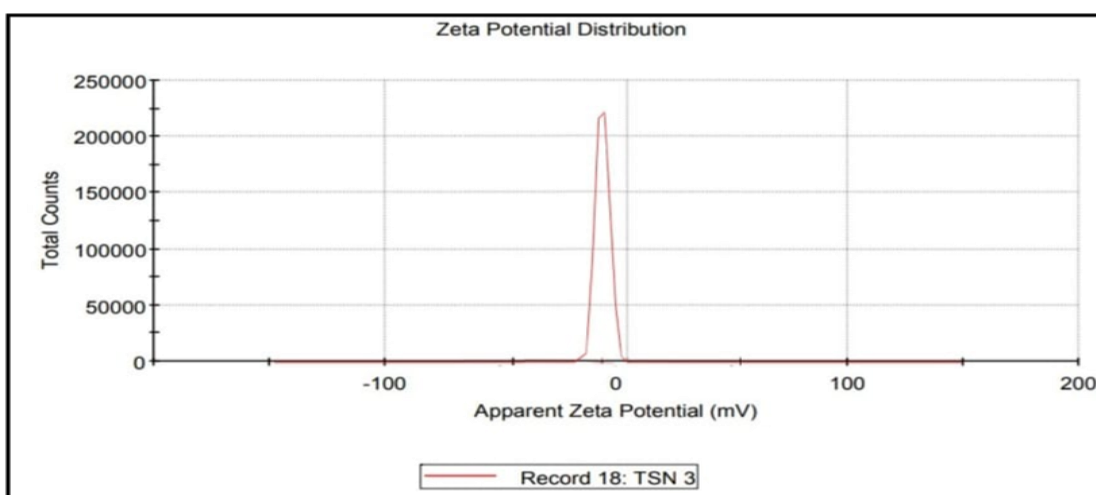


**Fig. 6B:** Zeta potential distribution of the synthesized silver nanoparticles

### 3.2.5. XRD Analysis

XRD analysis plays a major role in the characterization of the nanoparticles for identifying the structure and crystalline nature of the particle. The XRD pattern of the green synthesized *Tabebuia pallida* nanoparticles shows various diffraction peaks at  $2\theta = 32.20, 38.08, 46.18, 54.80$  corresponds to the (111), (200), (120) and (202) planes respectively (Fig. 7A and 7B). These diffraction patterns indicate the presence of face centered cubic crystalline structure of the synthesized nanoparticles. Our results very well coincide with Hemlata *et al.*, (2020) who carried out biosynthesis of silver nanoparticles Using *Cucumis prophetarum* aqueous leaf extract [29]. The other peaks at  $2\theta = 21.60, 27.82$  and  $57.47$  are the biomolecules present in the nanoparticles as a capping agent [30].

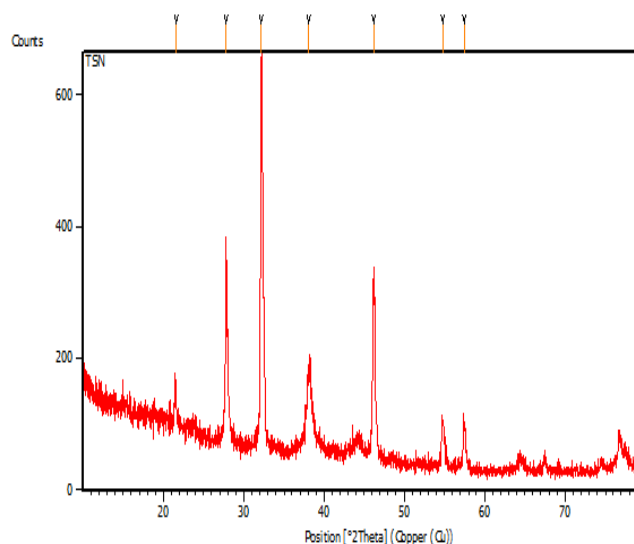


**Fig. 7A**

| S.No. | Pos. [° 2Th.] | Height [cts] |
|-------|---------------|--------------|
| 1     | 21.6039       | 33.36        |
| 2     | 27.8273       | 300.69       |
| 3     | 32.2066       | 580.30       |
| 4     | 38.0854       | 124.06       |
| 5     | 46.1882       | 262.71       |
| 6     | 54.8036       | 67.08        |
| 7     | 57.4705       | 68.09        |

Fig. 7B

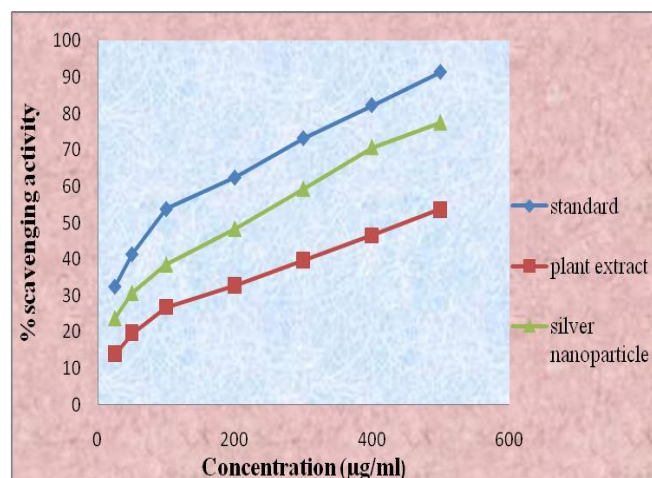
**Fig. 7A: XRD diffraction pattern of the synthesized silver nanoparticles, Fig.7B: 2 $\theta$  position and height of the spectrum**

### 3.3. In-vitro Free Radical Scavenging Assays

#### 3.3.1. DPPH Radical Scavenging Assay

The DPPH scavenging ability of the antioxidants is mainly due to the donation of hydrogen bond to the free radical. The plant phytochemicals like terpenoids, flavonoids, phenols and other phytoconstituents in the synthesized silver nanoparticles as a capping agent plays a major role in the scavenging of DPPH radicals. Initially the DPPH solution was purple in color and when exposed to the nanoparticles, it turns yellow due to acceptance of hydrogen. This clearly indicates the scavenging potential of the synthesized nanoparticles against DPPH [31]. The results of the DPPH scavenging ability of synthesized silver nanoparticles and *Tabebuia pallida* leaf extract are comparable with that of the standard quercetin is shown in the graph below (Fig. 8). From the graph it could be concluded that DPPH scavenging ability increases with increase in concentration of the AgNPs, Plant extract and quercetin. Notably, AgNPs exhibited highest scavenging ability of 77.63% in its highest concentration i.e. 500  $\mu\text{g/ml}$ , whereas the plant extract and quercetin exhibited 53.77% and 91.52% scavenging potential in the same concentration. The  $\text{IC}_{50}$  value of the silver nanoparticles and plant extract was found to be 227.82  $\mu\text{g/ml}$  and 439.23  $\mu\text{g/ml}$  and  $\text{IC}_{50}$  for quercetin was 118  $\mu\text{g/ml}$ .

Our results are in accordance with the previously published results of Arumugam *et al.*, who carried out green synthesis of silver nanoparticles from *Lippia nodiflora* aerial extract and found that the DPPH scavenging ability was found to be increased with increase in concentration of the sample. AgNPs showed highest scavenging of 67% at 500  $\mu\text{g/ml}$  and the standard exhibited 83% scavenging at the same concentration [32].



The values are represented as  $\pm\text{SD}$  for triplicates in each category,  $P$  value  $< 0.05$

**Fig. 8: DPPH radical scavenging activity of the silver nanoparticles**

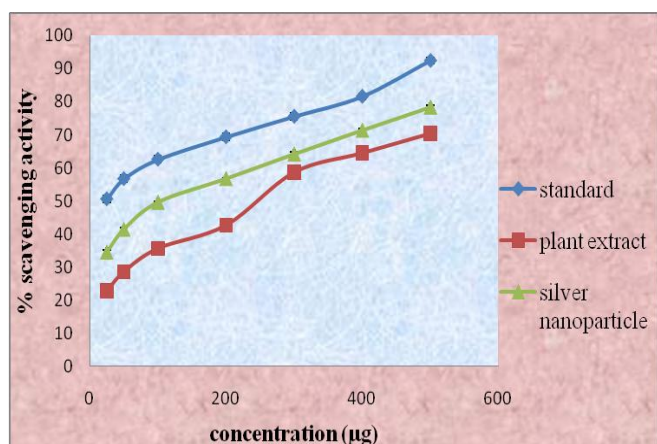
#### 3.3.2. ABTS radical scavenging assay

ABTS radical scavenging assay was mainly used to determine the radical scavenging ability of both chain-breaking and hydrogen ion donating antioxidants [33]. The ABTS scavenging ability of the AgNPs and Quercetin was expressed in the graph (Fig.9). The ABTS scavenging ability was increased with increase in concentration of both samples and standard. The scavenging ability of AgNPs was 34.64- 78.47% at a concentration range of 25-500  $\mu\text{g/ml}$ , for standard it was 50.56- 92.39 % and for the plant extract it was 22.77- 70.54 % in the same concentration. The  $\text{IC}_{50}$  value was found to be more for the AgNPs (148.23  $\mu\text{g/ml}$ ) and plant extract (264.3  $\mu\text{g/ml}$ ) and is comparatively less for the standard (24.56  $\mu\text{g/ml}$ ). In line with our study pooja *et al.*, synthesized silver nanoparticles using *Cassia roxburghii* leaf extract and found that the scavenging ability was increased with increase in concentration of the sample and achieved a highest scavenging potential of 73% in its highest concentration [34].

#### 3.3.3. Hydroxyl radical scavenging activity

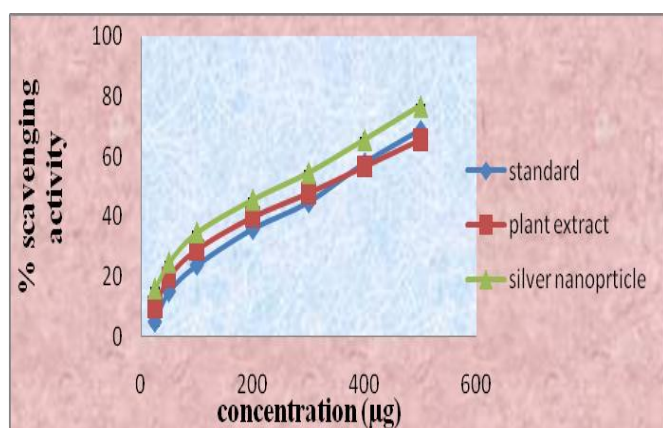
The hydroxyl radical scavenging activity of the synthesized silver nanoparticles, plant extract and standard quercetin was expressed in the Fig.10. The hydroxyl radical scavenging potential of the AgNPs is mainly due to the phenolic compounds that are responsible for the reduction of silver ions [35]. In our study, it was found that the hydroxyl radical scavenging potential increases with increase in concentration of the

sample. The hydroxyl radical scavenging potential of the AgNPs (76.78% at a concentration of 500 $\mu\text{g}/\text{ml}$ ) was found to be higher than that of the standard quercetin (68.70% at a concentration of 500 $\mu\text{g}/\text{ml}$ ) whereas the plant extract showed 65.62% scavenging effect against hydroxyl radicals. The  $\text{IC}_{50}$  value of AgNPs was found to be 264.78 $\mu\text{g}/\text{ml}$  and for the standard it was 339.27 $\mu\text{g}/\text{ml}$ . These results indicate that the hydroxyl radical scavenging ability of the AgNPs was very strong when compared to that of the standard quercetin. Our study was supported by a study carried out by Anand *et al.*, who synthesized silver nanoparticles from *Cestrum nocturnum* and carried out hydroxyl radical scavenging activity and found that the hydroxyl radical scavenging potential of the synthesized silver nanoparticles was found to be higher than that of the standard [36].



The values are represented as  $\pm\text{SD}$  for triplicates in each category,  $P$  value  $< 0.05$

**Fig. 9: ABTS radical scavenging activity of the silver nanoparticles**

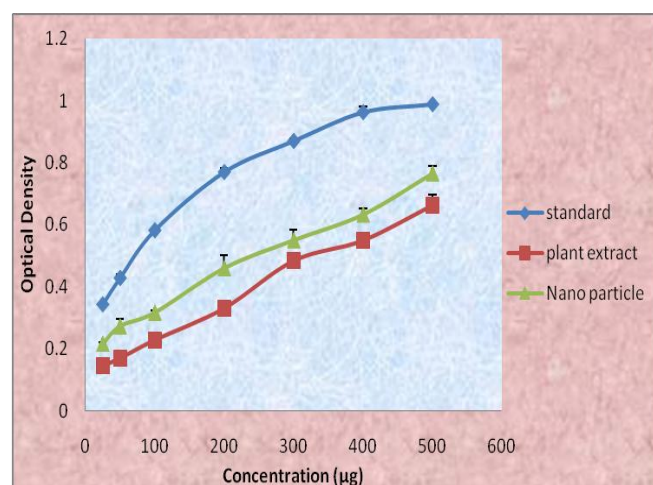


The values are represented as  $\pm\text{SD}$  for triplicates in each category,  $P$  value  $< 0.05$

**Fig. 10: Hydroxyl radical scavenging activity of the synthesized silver nanoparticles**

### 3.3.4. Reducing Power assay

The compounds which have the reducing ability will react with potassium ferricyanide and convert it to potassium ferrocyanide, this potassium ferrocyanide then reacts with ferric chloride and produces ferric-ferrous complex which can be measured at 700nm [37]. In the present study, it was found that the reducing power of plant extract, silver nanoparticle and the standard increases with increase in concentration (Fig. 11). The reducing ability of the standard quercetin was higher when compared to the AgNPs and plant extract. In line with our study Bhakya *et al.* synthesized silver nanoparticles from *Helicteres isora* and carried out various antioxidant assays. From their study it was found that the reducing ability of both standard and silver nanoparticles increases with increase in concentration [38].



The values are represented as  $\pm\text{SD}$  for triplicates in each category,  $P$  value  $< 0.05$

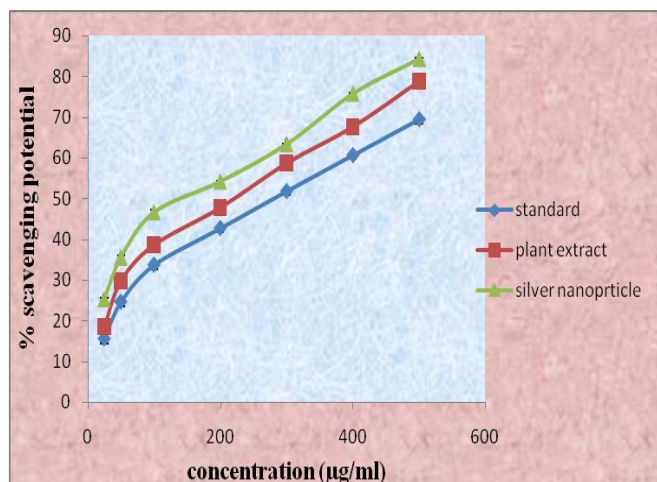
**Fig. 11: Reducing power assay for the synthesized silver nanoparticles**

### 3.3.5. Nitric oxide radical scavenging assay

Increased production of nitric oxide in the body leads to several disease complications [39]. So, excess nitric oxide should be scavenged by the antioxidants to maintain a healthy homeostasis. In our study, it was found that the nitric oxide radical scavenging ability increases with increase in concentration (Fig.12). The scavenging ability of AgNPs was 25.33%- 84.33% at a concentration range of 25-500  $\mu\text{g}/\text{ml}$ , for plant extract it was 18.57%- 78.77% and for standard it was 15.51 %- 69.45 % in the same concentration. The  $\text{IC}_{50}$  value was found to be less for the AgNPs (181.49  $\mu\text{g}/\text{ml}$ ) and comparatively more for the standard (295.71 $\mu\text{g}/\text{ml}$ ).



Our study was supported by Rajeshwari *et al* who carried out nitric oxide assay for the green synthesized silver nanoparticles from *Aegle marmelos* leaf extract and found that the scavenging potential of silver nanoparticles increases with increase in concentration [40].



The values are represented as  $\pm$ SD for triplicates in each category, *P* value < 0.05

**Fig. 12: Nitric oxide radical scavenging ability of the synthesized silver nanoparticles**

#### 4. CONCLUSION

Sunlight mediated green synthesis of silver nanoparticles was carried out using *Tabebuia pallida* leaf extract. The color change of the reaction mixture indicates the formation of silver nanoparticles. The synthesized silver nanoparticles were further characterized by UV-visible spectroscopy, Fourier transform infrared spectroscopy (FTIR) analysis, Field Emission Scanning Electron Microscope (FESEM), Dynamic Light Scattering (DLS), x-ray diffraction (XRD). The surface Plasmon resonance of the synthesized silver nanoparticles in UV-visible spectroscopy occur around 450 nm which is the main characteristic of the silver nanoparticles. FTIR spectral studies showed the presence of various functional groups of secondary metabolites which acted as a reducing and capping agent in the mechanism of silver nanoparticles synthesis. FESEM along with EDAX indicates that the average size of the synthesized nanoparticles is around 38.82 nm and is uniformly spherical in shape with very less agglomeration and the percentage weight of Ag was found to be 65.94. In DLS analysis it is observed that the average size of the nanoparticles was 55.4 nm with a Polydispersity Index (PDI) of 0.33 and the zeta potential was found to be -

15.6 mV. XRD analysis confirms that the synthesized nanoparticles are face centered cubic crystalline structure compared with the standard powder diffraction card. Furthermore the green synthesized silver nanoparticles were evaluated for their free radical scavenging activity using DPPH Radical Scavenging Assay, ABTS radical scavenging assay, Hydroxyl radical scavenging activity, Reducing Power assay and Nitric oxide radical scavenging assay compared with the standard antioxidant Quercetin. The silver nanoparticles, plant extract and standard quercetin exhibited a dose dependent scavenging potential

#### 5. ACKNOWLEDGEMENTS

The authors are thankful to the Department of Biochemistry, Biotechnology and Bioinformatics and Advanced Research Laboratory, Avinashilingam Institute for Home Science and Higher Education for Women for providing laboratory facilities.

#### Conflict of interest

None declared

#### 6. REFERENCES

- Rawan N, Kahtani A. *Saudi Dent J*, 2018; **30**:2107-2116.
- Vanshika R, Anjna S, Vijay PB, Raghvendra PS, Indresh KM. *Materials Today: Proceedings*, 2020; **29 Suppl 3**:911-916.
- Banerjee P, Satapathy M, Mukhopahayay A, *et al*. *Bioresour. Bioprocess*, 2014; **1(3)**:516-524.
- Kumar V, Gundampati RK, Singh DK, *et al*. *Ind. Eng. Chem. Res.*, 2016; **37**:224-236.
- Arumugam S, Jeyaraman J, Pappu S. *Resource-Efficient Technologies*, 2017; **3 Suppl 4**:506-515.
- Jiménez-González FJ, Veloza, LA, Sepúlveda-Arias JC. *Univ Sci.*, 2013; **18**:257-267.
- Mounil M, Ghanshyam P, Dimpy P, Parthvi P, Armi P. *Arabian Journal of Chemistry*, 2020; **13 Suppl 1**:2865-2872.
- Rautela A, Rani J, Debnath M. *J Anal Sci Technol*, 2019;**10**:5.
- Brand-williams W, Cuvelier ME, Berset C. *Lebensmittel Wissenschaft und Technologie*, 1995; **28(1)**:25-30.
- Shirwaikar Annie, Rajendran K, Kumar D. *Indian Journal of Experimental Biology*, 2004; **142**:803.
- Klein SM, Cohen G, Cederbaum AI. *Biochemistry*, 1991; **20**:6006-6012.
- Yildırım A, Oktay MV, Bilalog<sup>v</sup> lu. *Turk. J. Med. Sci.*, 2001; **31**:23-27.

13. Shirwaikar Annie, somashekar AP. *Indian J pharm Sci.*, 2003; **65**:68.
14. Sreejayan N Rao MNA. *J Pharm Pharmacol.*, 1997; **49**:105.
15. Veerasamy R, Xin TZ, Gunasagaran S, Xiang TFW, Yang, Jeyakumar N, et al. *Journal of Saudi Chemical Society*, 2011; **15**:113-120.
16. Vasireddy R, Paul R, Krishna Mitra A. *Nanomaterials and Nanotechnology*, 2012; **2**:8.
17. Marslin G, Siram K, Maqbool Q, et al. *Materials*, 2018; **11(6)**:940.
18. Banerjee P, Satapathy M, Mukhopahayay A, Das P. *Bioresour. Bioprocess*, 2014; **1**:1-10.
19. Raut Rajesh W, Lakkakula Jaya R, Kolekar Niranjan S, Mendhulkar Vijay D, Kashid Sahebrao B. *Curr. Nanosci.*, 2009; **5**:117-122.
20. Pirtarighat S, Ghannadnia M, Baghshahi S. *J Nanostruct Chem*, 2019; **9**:1-9.
21. Ajitha B, Reddy YAK, Reddy PS. *Spectrochimica Acta*, 2014; **121**:164-172.
22. Narayanan KB, Sakthivel N. *Mater. Res. Bull.*, 2011; **146**:1708-1713.
23. Vanaja M, Gnanajobitha G, Paulkumar K, Rajesh kumar S, Malarkodi C, Annadurai G. *J. Nanostruct. Chem.*, 2013; **3**:1-8.
24. Priya MN, Selvi BK, Paul JAJ. *Dig J Nanomater Biostructs.*, 2011; **6(2)**:869-877.
25. Sathishkumar G, Gobinath C, Karpagam K, Hemamalini V, Premkumar K, Sivaramakrishnan S. *Coll Surf B*, 2012; **95**:235-240.
26. Kaviya S, Santhanalaksnmi J, Viswanathan B, Muthumany J, Srinivasan K. *Spectrochim Acta*, 2011; **79**:594-598.
27. Susan A, Cumberland, Jamie R. *Journal of Chromatography A*, 2009; **1216 Suppl 52**: 9099-9105,
28. Anandalakshmi K, Venugobal J, Ramasamy V. *Applied Nanoscience*, 2015; **6(3)**:399-408
29. Hemlata, Prem RM, Arvind PS, Kiran KT. *ACS Omega*, 2020; **5(10)**:5520-5528.
30. Tahir Rasheed, Muhammad Bilal, Chuanlong Li, Faran Nabeel, Muhammad Khalid, Hafiz MN Iqbal. *J Photochem Photobiol B*, 2018; **181**:44-52.
31. Guntur SR, Kumar NS, Hegde MM, Dirisala VR. *Analytical chemistry insights*, 2018; **13**:1-9.
32. Arumugam Sudha, Jeyaraman Jeyakanthan, Pappu Srinivasan. *Resource-Efficient Technologies*, 2017; **3(4)**:506-515.
33. Leong LP, Shui G. *Food Chem*, 2012; **76**:69-75.
34. pooja Moteriy, Hemali Padalia, Sumitra Chanda. *Journal of Genetic Engineering and Biotechnology*, 2017; **15(2)**:505-513.
35. Sundararajan B, Mahendran G, Thamaraiselvi R, Ranjitha Kumari BD. *Bull. Mater. Sci.*, 2016; **39(2)**: 423-431.
36. Anand KK, Ragini S, Payal S, Virendra BY, Gopal N. *Journal of Ayurveda and Integrative Medicine*, 2020; **11(1)**:37-44.
37. Bhalodia, NR, Nariya PB, Acharya RN, Shukla VJ. *Ayu*, 2013, **34(2)**:209-214.
38. Bhakya S, Muthukrishnan S, Sukumaran M, et al. *Appl Nanosci*, 2016; **6**:755-766.
39. Sun T, Ho CT. *Food Chemistry*, 2005; **90**:743-749.
40. Rajeshwari et al. *Indo Am. J. Pharm. Sci*, 2015; **2(10)**: 1453-1459.